SIMS proceedings paper

SURFACE and INTERFACE ANALYSIS

Received: 30 September 2011 Revised: 17 January 2012 Accepted: 21 March 2012 Published online in Wiley Online Library: 20 April 2012

(wileyonlinelibrary.com) DOI 10.1002/sia.5009

Characteristics of positive and negative secondary ions emitted from Au_3^+ and Au_{400}^{+4} impacts

J. D. DeBord,[a] F. A. Fernandez-Lima,[a] S. V. Verkhoturov,[a] E. A. Schweikert[a]* and S. Della-Negra[b]

The current limitation for SIMS analyses is insufficient secondary ion yields, due in part to the inefficiency of traditional primary ions. Massive gold clusters are shown to be a route to significant gains in secondary ion yields relative to other commonly used projectiles. At an impact energy of 520 keV, Au_{400}^{+4} is capable of generating an average of greater than ten secondary ions per projectile, with some impact events generating >100 secondary ions. The capability of this projectile for signal enhancement is further displayed through the observation of up to seven deprotonated molecular ions from a single impact on a neat target of the model pentapeptide leu-enkephalin. Positive and negative spectra of leu-enkephalin reveal two distinct emission regimes responsible for the emission of either intact molecular ions with low internal energies or small fragment species. The internal energy distribution for this projectile is measured using a series of benzylpyridinium salts and compared with the small polyatomic projectile Au_3^+ at 110 keV as well as distributions previously reported for electrospray ionization and fast atom bombardment. These results show that Au_{400}^{+4} offers high secondary ion yields not only for small fragment ions, e.g. CN^-, typically observed in SIMS analyses, but also for characteristic molecular ions. For the leu-enkephalin example, the yields for each of these species are greater than unity. Copyright © 2012 John Wiley & Sons, Ltd.

Supporting information may be found in the online version of this article.

Keywords: Cluster-SIMS; ion yield; internal energy; peptide fragmentation; leu-enkephalin; angiotensin

Introduction

Much current research in the field of SIMS focuses on the issue of insufficient secondary ion (SI) yields for trace or imaging analyses. Attempts to address this problem have been directed at either enhancing the ionization probability of sputtered species through the addition of a matrix, such as cesium,[1] water clusters,[2] ionic liquids,[3] or glycerol,[4] or improving the general SI yield through the use of novel primary ions (PIs), such as C_{60},[5] water clusters,[6] argon clusters,[7] or metal clusters.[8,9] Massive gold clusters have previously been proven as a path to improved SI yields.[10] This research seeks to further display the efficiency of the Au_{400}^{+4} projectile at high impact energies as well as address concerns regarding the fragmentation of SIs created by Au_{400}^{+4} impacts at these higher energies. Recent work in our laboratory has focused on the incorporation of a new Pegase 120 kV PI platform developed at the Institut de Physique Nucléaire d'Orsay into our custom-built SIMS instrument. The present work reports molecular and fragment ion yields for the model pentapeptide leu-enkephalin, a well-known calibration standard in mass spectrometry, as well as angiotensin fragments I, II, and III at this new impact energy. The extensive characterization of leu-enkephalin fragmentation enables its use as a measure of the internal energy imparted to the molecule from various ionization methods and experimental parameters.[11] To further address the internal energy distribution expected for massive metal cluster impacts, we utilize the survival yield method proposed by De Pauw *et al.*[12] to measure the internal energy distributions of Au_{400}^{+4} and Au_3^+. These results are compared with distributions previously measured for other ionization techniques.

Experimental section

Materials

Chemicals for the preparation of neat peptide targets and 1-(4-nitrobenzyl)pyridinium bromide were purchased from Sigma Aldrich (St. Louis, MO). 1-(4-Methoxyphenyl)methylpyridinium tetrafluoroborate, 1-(4-methylphyenyl)methylpyridinium bromide, and 1-(4-chlorophenyl)methylpyridinium chloride were purchased from the Florida Center for Heterocyclic Compounds (Gainesville, FL), and 1-(4-cyanobenzyl)pyridinium chloride was purchased from Otava (Toronto, Ontario). Solutions (1 mg/ml) of each peptide and benzylpyridinium salts in 1 : 1 MeOH/H_2O were electrospray deposited in atmosphere onto either stainless steel supports (negative mode) or gold-coated silicon wafers (positive mode) from Silicon Valley Microelectronics (Santa Clara, CA). The substrates were chosen to eliminate spectral interferences because each displays limited ion emission in their respective polarities. Parallel samples of the benzylpyridinium salts were also prepared by dropcasting 20 μl of the 1 mg/ml solutions onto gold-coated silicon wafers to monitor the effect of sample preparation on measured survival yields.

* *Correspondence to: E. A. Schweikert, Texas A&M University, College Station, TX 77843, USA.*
E-mail: schweikert@chem.tamu.edu

a *Texas A&M University, College Station, TX 77843, USA*

b *Institut de Physique Nucléaire d'Orsay, UMR 8608, Université Paris Sud, F91406 Orsay Cedex, France*

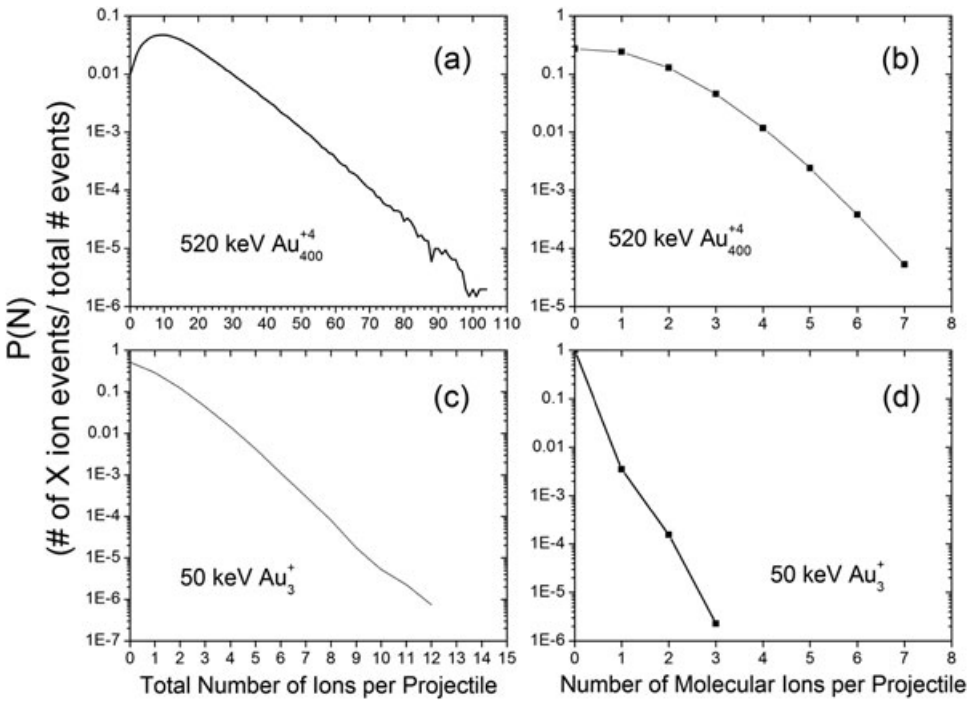

Figure 1. Total secondary ion multiplicity distributions for (a) 520 keV Au_{400}^{+4} and (b) 520 keV Au_{400}^{+4} and (c) 50 keV Au_3^+ and molecular ion selected multiplicity distributions for (d) 50 keV Au_3^+ measured per projectile impact on a neat electrosprayed surface of leu-enkephalin. Results are obtained in negative mode and are not corrected for transmission efficiency.

Analysis

The experimental setup consists of a 120 qkeV gold liquid metal ion source (Au-LMIS) coupled to two analysis chambers, with the first chamber being used for negative SI detection and the second being used for positive SI detection. The current instrument and event-by-event detection methodology have been described in detail in Refs.[13,14] Briefly, an Au-LMIS capable of producing mass selected gold cluster beams (Au_n^{+q}, $n = 1$–1000, $q = 1$–10) is pulsed across an aperture to deliver single projectiles into an analysis chamber at a rate of ~1000 Hz. The electrons and ions generated from a cluster impact on the biased analytical surface are accelerated toward either a 1.7 m drift tube with a dual-stage reflectron (negative chamber, 60% transmission efficiency) or a 1.0 m linear drift tube (positive chamber, 90% transmission efficiency). Electrons (negative mode) or protons (positive mode) are turned by a weak magnetic field toward a chevron-style microchannel plate detector. Detection of these light species indicates that an impact has occurred, and the signal serves as a start for the time-of-flight measurement. SIs are detected in pulse counting mode using an eight-anode chevron-style microchannel plate detector to allow for the detection of up to eight isobaric ions per event. All data shown represent spectra with ~10^6 impact events where each event refers to the detection of all SIs originating from a single PI impact.

Results

The total SI and molecular ion multiplicity plots for 520 keV Au_{400}^{+4} impacts on leu-enkephalin (555.6 amu) are shown in Fig. 1a and 1b, respectively. The total ion multiplicity is a measure of the number of SIs detected per impact event. This plot shows that the mean number of ions detected per impact on a neat leu-enkephalin surface is 13.3. The Poisson distribution extends out to events containing ~100 SIs per event. Figure 1b shows the number of leu-enkephalin deprotonated molecular ions (m/z 554.6) detected per impact. Significant yields are observed for multiple molecular ion emission events, with some events generating as many as seven molecular ions. Such high yield events are unique to massive cluster impacts, as shown by the corresponding plots for 50 keV Au_3^+ in Fig. 1c and 1d. For Au_3^+, the average number of SIs detected per projectile is only 0.76. It is also important to note that the figures given are not corrected for transmission efficiency, which is 60% for this setup.

Representative negative (Fig. 2a) and positive (Fig. 2b) ion spectra for leu-enkephalin are characterized by the abundant emission of intact molecular ion signals (transmission corrected yield of 1.7 in negative mode) as well as abundant small fragment

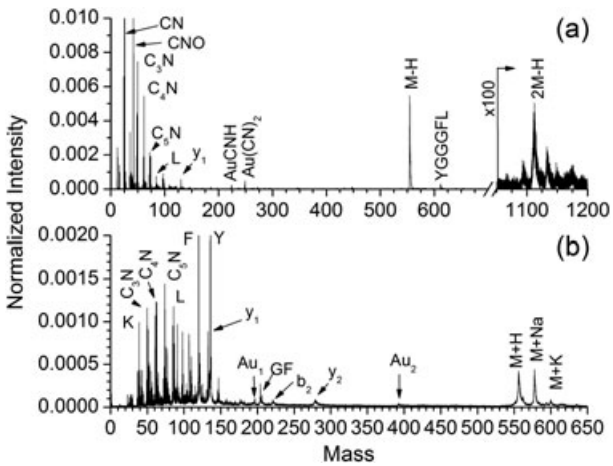

Figure 2. (a) Negative and (b) positive mass spectra for a neat electrosprayed surface of leu-enkephalin analyzed by 520 keV and 440 keV Au_{400}^{+4} projectiles, respectively.

Table 1. SI yields for various negative ions obtained from impacts of 520 keV Au_{400}^{+4} on neat targets of angiotensins I, II, and III and leu-enkephalin

	Angiotensin I		Angiotensin II		Angiotensin III		Leu-enkephalin	
Ion	Mass	Yield	Mass	Yield	Mass	Yield	Mass	Yield
M-H	1295	2.09E-2	1045	4.35E-2	931	9.24E-1	554	1.69
2 M-H	—	—	—	—	1860	1.93E-3	1109	4.25E-2
CN	26	1.18	26	1.74	26	1.93E-2	26	2.14
P/R	68	8.51E-3	68	2.23E-2	68	1.48E-2	—	—
V	70	1.17E-2	70	3.15E-2	70	6.41E-3	—	—
I/L	84	2.61E-2	84	6.19E-2	84	3.92E-2	84	6.74E-2
D	86	1.31E-2	86	3.41E-2	—	—	—	—
R	98	2.46E-2	98	6.07E-2	—	—	—	—
H	108	1.86E-2	108	3.91E-2	108	2.04E-2	—	—
F	—	—	118	5.53E-2	118	1.34E-2	118	1.54E-2
P	—	—	124	1.19E-2	124	2.99E-2	—	—
Y	—	—	134	3.01E-2	134	1.24E-2	134	1.76E-2
y_1	—	—	164	9.79E-3	—	—	130	9.31E-2
a_2-NH_3	—	—	225	5.72E-3	—	—	—	—
y_2	—	—	261	9.04E-3	—	—	—	—
Y_2	265	7.94E-3	—	—	—	—	—	—
b_2	—	—	—	—	—	—	219	5.23E-3

Data corrected for 60% transmission efficiency.

ions (<200 amu), including peaks corresponding to atomized products such as CN^- (transmission corrected yield of 2.1 in negative mode) and individual amino acid residues L, F, and Y. Peaks corresponding to backbone fragmentation are curiously absent from the 200–500 mass region of the two spectra with the exception of the b_2 and y_2 fragments observed in positive mode. This observation is replicated for other peptides analyzed (data not shown). Negative ion yields for angiotensins I, II, III, and leu-enkephalin are given in Table 1. All recognizable fragments are included, although none of these are beyond 300 amu. Peptide fragmentation has long been recognized as a gauge of the internal energy imparted during the ion formation process.[11,15] In this capacity, higher internal energies result in a lower molecular ion survival rate and enhanced fragment ion production. Typically, amino acid residues are only observed in the spectrum as a result of multistep fragmentation processes because two bonds must be cleaved to liberate the internal fragments. These elaborate fragmentation mechanisms often observed in collision- or surface-induced dissociation spectra necessitate the survival of many species along the fragmentation tree.[11] The observation of internal fragments without the corresponding parent ions suggests that these ions do not originate from traditional gas-phase fragmentation processes but are instead formed under the high-temperature/high-pressure conditions within the projectile track. Molecular dynamics simulations have shown that the energy densities which develop within the track and at the crater rim are quite different.[16] Such simulations as well as experimental results have shown that molecular ion emission occurs from the rim of the impact crater resulting in ions with internal energies sufficiently low that they survive for analysis.[17,18]

To address the question of how much internal energy is imparted to SIs by the massive gold cluster projectile, we have measured the internal energy distribution using a series of benzylpyridinium salts according to the survival yield method proposed in Refs.[12,19,20] This method for determining the internal energy distribution entails measuring the survival yields of multiple thermometer ions, each having a different critical energy for fragmentation. Benzylpyridinium ions are chosen because (1) their fragmentation proceeds almost exclusively along a single pathway (see Supplementary Fig. 1), (ii) the activation energy for fragmentation of each molecule differs according to the electron donating/withdrawing properties of the substituent group on the benzene ring (see Supplementary Table 1), and (iii) the structures and masses of all thermometer molecules are similar. By plotting the ratio of molecular ion peak intensity to the sum of molecular and fragment ion intensities $\{I(M^+) / [I(M^+) + I(F^+)]\}$, which is defined as the survival yield, *versus* the calculated bond energy of the

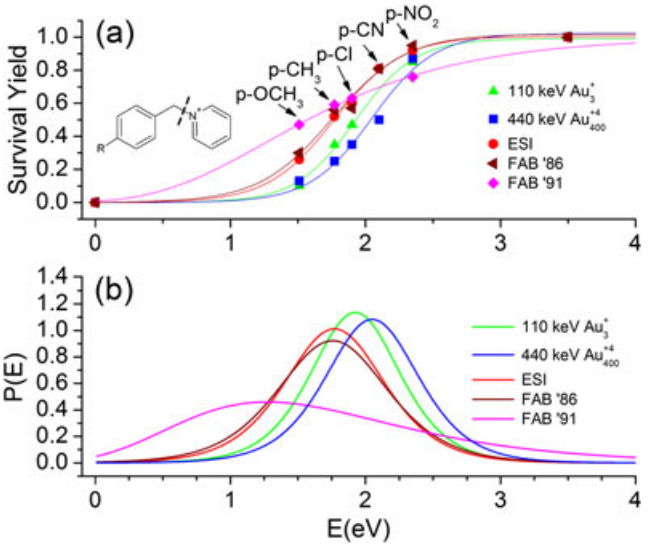

Figure 3. (a) Breakdown curves and (b) internal energy distributions for various ionization techniques. Inset shows the generic benzylpyridinium ion structure as well as the bond which undergoes fragmentation. Each thermometer ion differs by the replacement of the –R substituent group. ESI data from Ref.[21] are reproduced with permission from Elsevier. The 1991 FAB data from Ref.[20] are reproduced with permission from Wiley-Blackwell. The 1986 FAB data taken from Ref.[19] are reproduced with permission from Springer Science+Business Media.

fragmented bond, we obtain a breakdown curve. This quantity characterizes the internal energies imparted to each molecule. Boundary conditions are assumed where the survival yield for theoretical molecules having critical bond energies of 0 and 3.5 eV would have survival yields of 0 and 1, respectively.[12] These data points can be fitted with a sigmoidal curve, and differentiation of this curve gives the distribution of internal energies which are accumulated on the fragmented bond. Figure 3a shows the survival yield plots along with their sigmoidal fits for the electrosprayed samples analyzed with 440 keV Au_{400}^{+4} and 110 keV Au_3^+. Survival yields obtained from samples prepared by dropcasting (data not shown) are similar, showing in this case that the sample preparation method does not influence the resultant internal energy distributions. Also plotted are previous data from the literature acquired using electrospray ionization (ESI)[21] and fast atom bombardment (FAB).[19,20] The resultant internal energy distributions for the various ionization methods are shown in Fig. 3b. The ESI and FAB experiments serve as references for well-recognized methods of "soft" ionization. The interesting feature common to all data except the FAB data from Ref.[20] is that they each have narrow internal energy distributions spanning from approximately 1 to 3 eV. The FAB data from Ref.[20] displays a much broader internal energy distribution, which tails off to much higher energies than do the other plots shown. The differences between the two sets of FAB data are not addressed in the literature but can likely be attributed to differences in experimental conditions. The positions of each distribution along the energy axis should be considered qualitative such that ions formed from Au_3^+ and Au_{400}^{+4} impacts have relatively higher internal energies as compared with ESI and FAB. The kinetic shift calculations proposed in Refs.[12,22] to render these data quantitative are beyond the scope of this study. The current calculation is assumed to underestimate the actual internal energy distributions for Au_3^+ and Au_{400}^{+4} impacts, although the relative comparisons to ESI and FAB are maintained with such a systematic error. The similarity between these distributions is rather surprising considering the high energy densities created by the impacting projectiles. The narrow internal energy distribution for SIs produced from Au_{400}^{+4} impacts confirms the observation from peptide spectra that molecular ion emission results from a "soft" desorption/ionization mechanism. The fact that the Au_{400}^{+4} distribution is shifted relative to FAB is also significant because these previous articles suggested that the extraction of analyte species from liquid matrices rather than solid surfaces reduces the internal energies of SIs. The present results support this prediction.

Conclusion

The fragmentation of leu-enkephalin and the internal energy distributions measured offer an assessment of the internal energy transferred to SIs from Au_{400}^{+4} impacts. This distribution is narrow and similar to the one measured for ESI, which is a standard for "soft" ionization. Taken with the high SI yields reported earlier, the Au_{400}^{+4} projectile allows for the incorporation of both "soft" ionization conditions and high analytical sensitivity into a surface analysis tool.

Acknowledgements

The authors acknowledge the financial support from the National Science Foundation (Grant CHE-0750377). F.A.F.-L. acknowledges support from the National Institute of Health (Grant 1K99RR030188-01), and J.D.D. acknowledges a fellowship from the US Department of Homeland Security.

References

[1] T. Wirtz, H. N. Migeon, *Appl. Surf. Sci.* **2004**, *222*, 186.
[2] G. Li, J. Cyriac, L. Gao, R. Graham Cooks, *Surf. Interface Anal.* **2011**, *43*, 498.
[3] J. J. D. Fitzgerald, P. Kunnath, A. V. Walker, *Anal. Chem.* **2010**, *82*, 4413.
[4] T. M. Brewer, C. Szakal, G. Gillen, *Rapid Commun. Mass Spectrom.* **2010**, *24*, 593.
[5] E. A. Schweikert, M. J. van Stipdonk, R. D. Harris, *Rapid Commun. Mass Spectrom.* **1996**, *10*, 1987.
[6] K. Mori, D. Asakawa, J. Sunner, K. Hiraoka, *Rapid Commun. Mass Spectrom.* **2006**, *20*, 2596.
[7] N. Toyoda, J. Matsuo, T. Aoki, I. Yamada, D. B. Fenner, *Appl. Surf. Sci.* **2003**, *203–204*, 214.
[8] R. D. Rickman, S. V. Verkhoturov, E. S. Parilis, E. A. Schweikert, *Phys. Rev. Lett.* **2004**, *92*, 047601.
[9] R. D. Rickman, S. V. Verkhoturov, E. A. Schweikert, *Appl. Surf. Sci.* **2004**, *231–232*, 54.
[10] R. D. Rickman, S. V. Verkhoturov, G. J. Hager, E. A. Schweikert, J. A. Bennett, *Int. J. Mass Spectrom.* **2005**, *241*, 57.
[11] J. Sztaray, A. Memboeuf, L. Drahos, K. Vekey, *Mass Spectrom. Rev.* **2011**, *30*, 298.
[12] V. Gabelica, E. De Pauw, *Mass Spectrom. Rev.* **2005**, *24*, 566.
[13] S. Della-Negra, J. Arianer, J. Depauw, S. V. Verkhoturov, E. A. Schweikert, *Surf. Interface Anal.* **2011**, *43*, 66.
[14] F. A. Fernandez-Lima, V. T. Pinnick, S. Della-Negra, E. A. Schweikert, *Surf. Interface Anal.* **2011**, *43*, 53.
[15] A. Pak, D. Lesage, Y. Gimbert, K. Vékey, J.-C. Tabet, *J. Mass Spectrom.* **2008**, *43*, 447.
[16] A. Delcorte, B. J. Garrison, K. Hamraoui, *Anal. Chem.* **2009**, *81*, 6676.
[17] D. A. Brenes, B. J. Garrison, N. Winograd, Z. Postawa, A. Wucher, P. Blenkinsopp, *J. Phys. Chem. Lett.* **2011**, *2*, 2009.
[18] S. Della-Negra, J. Depauw, C. Guillermier, E. A. Schweikert, *Surf. Interface Anal.* **2011**, *43*, 62.
[19] E. De Pauw, G. Pelzer, J. Marien, P. Natalis, *Springer Proc. Phys.* **1986**, *9*, 103.
[20] F. Derwa, E. De Pauw, P. Natalis, *Org. Mass Spectrom.* **1991**, *26*, 117.
[21] M. Nefliu, J. N. Smith, A. Venter, R. G. Cooks, *J. Am. Soc. Mass Spectrom.* **2008**, *19*, 420.
[22] C. Collette, L. Drahos, E. De Pauw, K. Vékey, *Rapid Commun. Mass Spectrom.* **1998**, *12*, 1673.

